

## PHYSICS

# Correlation between scale-invariant normal-state resistivity and superconductivity in an electron-doped cuprate

Tarapada Sarkar<sup>1</sup>, P. R. Mandal<sup>1</sup>, N. R. Poniatowski<sup>1</sup>, M. K. Chan<sup>2</sup>, Richard L. Greene<sup>1\*</sup>

An understanding of the normal state in the high-temperature superconducting cuprates is crucial to the ultimate understanding of the long-standing problem of the origin of the superconductivity itself. This so-called “strange metal” state is thought to be associated with a quantum critical point (QCP) hidden beneath the superconductivity. In electron-doped cuprates—in contrast to hole-doped cuprates—it is possible to access the normal state at very low temperatures and low magnetic fields to study this putative QCP and to probe the  $T \rightarrow 0$  K state of these materials. We report measurements of the low-temperature normal-state magnetoresistance (MR) of the n-type cuprate system  $\text{La}_{2-x}\text{Ce}_x\text{CuO}_4$  and find that it is characterized by a linear-in-field behavior, which follows a scaling relation with applied field and temperature, for doping ( $x$ ) above the putative QCP ( $x = 0.14$ ). The magnitude of the unconventional linear MR decreases as  $T_c$  decreases and goes to zero at the end of the superconducting dome ( $x \sim 0.175$ ) above which a conventional quadratic MR is found. These results show that there is a strong correlation between the quantum critical excitations of the strange metal state and the high- $T_c$  superconductivity.

## INTRODUCTION

Quantum criticality has been a recurrent theme for attempting to understand the physics of the cuprates and other strongly correlated materials (1, 2). But, despite extensive theoretical and experimental effort over the past 30 years, the relation between quantum criticality and the anomalous properties of the normal state and the origin of the superconductivity is unresolved. There has been much experimental evidence for a quantum critical point (QCP) as a function of doping in both electron-doped (3, 4) and hole-doped (1, 5–7) cuprates. However, the nature of the phase for doping below the QCP is undetermined. For the n-type, the QCP is most likely associated with long- or short-range antiferromagnetic (AFM) order (with carrier  $\ell_{\text{mfp}} <$  magnetic correlation length), while for the p-type, the QCP marks the end of a pseudogap phase of unknown origin. The QCP in both cuprate types is associated with a Fermi surface reconstruction (FSR), where a large hole-like FS is found above the FSR doping (3, 4, 8–11) and a reconstructed FS of electron and hole pockets is found at lower doping. The FS reconstruction is observed in zero field in the n-doped cuprates (3); a large field is required in the p-doped cuprates. The normal-state transport properties near the QCP are quite different for n- and p-type cuprates. Above  $T_c$  (for  $H = 0$ ), hole-doped cuprates exhibit the mysterious linear-in- $T$  resistivity, which extends to high temperatures beyond the Mott-Ioffe-Regel (12) limit (so-called bad metal behavior). Above  $T_c$  ( $H = 0$ ), the electron-doped cuprates exhibit an equally mysterious  $\rho \sim T^2$  behavior extending to high temperature (800 to 1000 K) (13). A recent paper (14) has discussed this anomalous  $T \gg T_c$  resistivity in n-type and concluded that a non-Fermi liquid (FL) scattering related to strong interaction-induced hydrodynamics (driven by the underlying quantum criticality) is likely the cause. A concurrent study of the  $T \gg T_c$  thermal diffusivity of n-type cuprates (15) has also suggested that this high-temperature (above  $\sim 250$  K) transport is of hydro-

dynamic origin, i.e., nonquasiparticle transport of a fluid of electrons and phonons controlled by “Planckian” dissipation (16, 17).

The role of a magnetic field on the QCP and the normal-state properties is also undetermined despite much theoretical and experimental effort. The electron-doped cuprates have a much lower critical field ( $H_{c2} < 10$  T) (3, 18) than hole-doped cuprates, and this allows access to the very low-temperature ( $T \rightarrow 0$  K) normal-state properties. For example, Hall effect studies at 400 mK have suggested that the FSR occurs at a doping just above the doping for maximum  $T_c$  (optimal doping); 0.17 in  $\text{Pr}_{2-x}\text{Ce}_x\text{CuO}_4$  (PCCO) (4) and 0.14 in  $\text{La}_{2-x}\text{Ce}_x\text{CuO}_4$  (LCCO) (19), a conclusion confirmed by angle-resolved photoemission spectroscopy (3, 20) and quantum oscillation experiments for PCCO (21) and  $\text{Nd}_{2-x}\text{Ce}_x\text{CuO}_4$  (NCCO) (10). In addition, for fields just above  $H_{c2}$ , it was shown that a linear-in- $T$  resistivity extends from 10 K down to 30 mK in LCCO for the doping range of 0.14 to 0.17 and that the strength of this linear term correlates with the magnitude of  $T_c$  (22). The linear-in- $T$  resistivity—in contrast to the expectation of FL quadratic temperature dependence at these low temperatures—suggests a strong interaction between the metallic electrons and the critical fluctuations associated with the QCP.

What has not been studied (or understood) is how the magnetic field may affect these fluctuations and hence the low-temperature metallic state. In this work, we remedy this deficiency by measurements of the magnetoresistance (MR) in the normal state of LCCO in the same temperature and doping range ( $0.14 < x < 0.17$ ) where the linear-in- $T$  resistivity is found. We find a linear-in- $H$  behavior, a distinctly different response than for quasiparticles in conventional metals, where one expects an  $\text{MR} \sim H^2$  for fields where  $\omega_c \tau \ll 1$ . The magnitude of the linear-in- $H$  resistivity mirrors the magnitude and doping evolution of the linear-in- $T$  resistivity, with both going to zero at the end of the superconducting (SC) dome. Moreover, the temperature-dependent MR follows a scaling relation with applied field and temperature for doping ( $x$ ) above the QCP up to the end of the SC dome. This shows that there are excitations, common to both field and temperature, which are correlated with the superconductivity (and probably the cause).

Copyright © 2019  
The Authors, some  
rights reserved;  
exclusive licensee  
American Association  
for the Advancement  
of Science. No claim to  
original U.S. Government  
Works. Distributed  
under a Creative  
Commons Attribution  
NonCommercial  
License 4.0 (CC BY-NC).

<sup>1</sup>Center for Nanophysics and Advanced Materials and Department of Physics, University of Maryland, College Park, MD 20742, USA. <sup>2</sup>The National High Magnetic Field Laboratory, Los Alamos National Laboratory, Los Alamos, NM 87545, USA. \*Corresponding author. Email: rickg@umd.edu

## RESULTS

In Fig. 1 (A to C), we show the *ab*-plane MR at temperatures between 400 mK and 15 K for *c*-axis field up to 14 T, for LCCO thin films with doping  $x = 0.15, 0.16,$  and  $0.17$ . At low temperatures, the normal-state MR is linear in field for all doping. A linear-in- $H$  to quadratic-in- $H$  cross-over occurs at higher temperatures at low field ( $<15$  T), as shown in Fig. 2. The data show that the cross-over temperature decreases with increasing doping. Linear-in- $H$  MR exists to very low field for doping  $x = 0.15$  (20 K),  $x = 0.16$  (20 K), and  $x = 0.17$  ( $\sim 5$  K; see Fig. 1). The MR in  $x = 0.16$  at 20 K is almost linear down to zero field that is clear from the fitting  $\rho(H) = \rho(0) + C(x)(\mu_0 H)^n$ , where  $n = 1.13$ . The fact that  $n$  is not exactly 1 could result from a small quadratic-in- $H$  contribution. The magnitude of the  $H^2$  MR ( $<20$  T) decreases with temperature measured up to 80 K, as shown in Fig. 3 and fig. S1. Thus, at higher temperature, the transverse MR is similar to that found in conventional metals. However, the origin of the higher  $T$  MR is yet to be determined.

In Fig. 3, we show *ab*-plane MR at temperatures between 360 mK and 60 K for *c*-axis dc field up to 31 T for doping  $x = 0.15$  and  $0.16$ . In

the Supplementary Materials, fig. S5 shows the *ab*-plane MR for a second sample with 0.15 doping measured in pulsed field up to 65 T. The MR measured at the lowest temperature fits well with  $\Delta R \propto \mu_0 H$ . These high-field, unsaturated, linear-in- $H$  data strongly suggest that the low-field (up to 14 T; Fig. 1A) MR is not an SC fluctuation effect. The linear-in- $H$  data may continue to lower field, but the onset of superconductivity rules out a study of the normal-state transport properties for  $H < H_{c2}$ . However, the measured MR just above the transition temperature strongly suggests that linear-in- $H$  resistivity continues to a much lower field (see Figs. 2 and 3).

In Fig. 4, we show the linear-in-temperature resistivity coefficient  $A(x)$  and the linear-in-field resistivity coefficient  $C(x)$  obtained from fits to the low-temperature linear regions with  $\rho(T) = \rho_0 + A(x)T$  and  $\rho(H) = \rho(0) + C(x)(\mu_0 H)$ . Both  $A(x)$  and  $C(x)$  decrease with  $T_c$  as  $x$  increases, and both go to zero at the doping where the superconductivity ends. In the non-SC-overdoped regime, the resistivity varies as  $T^2$  (fig. S6), and the MR goes as  $H^2$  for  $T > 5$  K. A schematic temperature versus doping phase diagram in the inset of Fig. 5B summarizes the temperature- and field-dependent magnetotransport data of LCCO.

## DISCUSSION

These results are incompatible with that expected in conventional metals (23) where the MR from quasiparticles is controlled by the cyclotron frequency ( $\omega_c = e\mu_0 H/m^*$ ) and the relaxation time,  $\tau$ , i.e.,  $(\delta\rho/\rho(0)) \sim (\omega_c \tau)^2 \propto H^2$  in the limit where  $\omega_c \tau < 1$ . At 14 T and 400 mK, we estimate  $\omega_c \tau < 0.15 \pm 0.05$  for our LCCO films. We do observe an MR proportional to  $H^2$  at higher temperatures at low field (Figs. 1, 2, and 3 and fig. S1), where we also find (14)  $\rho$  proportional to  $T^2$ . This cross-over in transport behavior as a function of  $T$  is shown schematically in the inset of Fig. 5B. However, the high-field ( $>20$  T), high-temperature MR remains linear with field as shown in Fig. 3. Our results suggest scale-invariant transport (i.e., lack of an intrinsic energy scale), which is often associated with quantum criticality. To check for this, we try a scaling analysis similar to that proposed in (24) for a pnictide at a QCP. In Fig. 5A, we plot  $\Delta\rho = (\bar{\rho} - \bar{\rho}(0))/T$  versus  $\mu_0 H/T$  [where  $\bar{\rho} = \frac{\rho(H,T)}{\rho(0,200)}$ ] is normalized with  $\rho(0,200)$  to avoid any geometrical

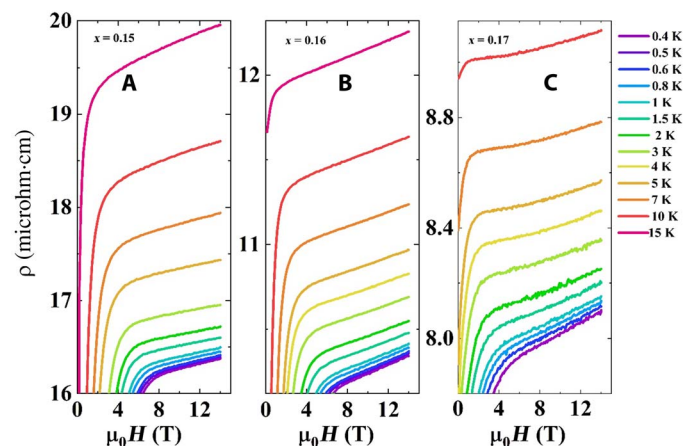


**Fig. 1. MR versus doping.** Magnetoresistivity for LCCO thin films with  $x = 0.15, 0.16,$  and  $0.17$ . (A to C) *ab*-plane transverse resistivity versus magnetic field ( $H//c$  axis) as a function of temperature (color solid lines) for all  $x$ .

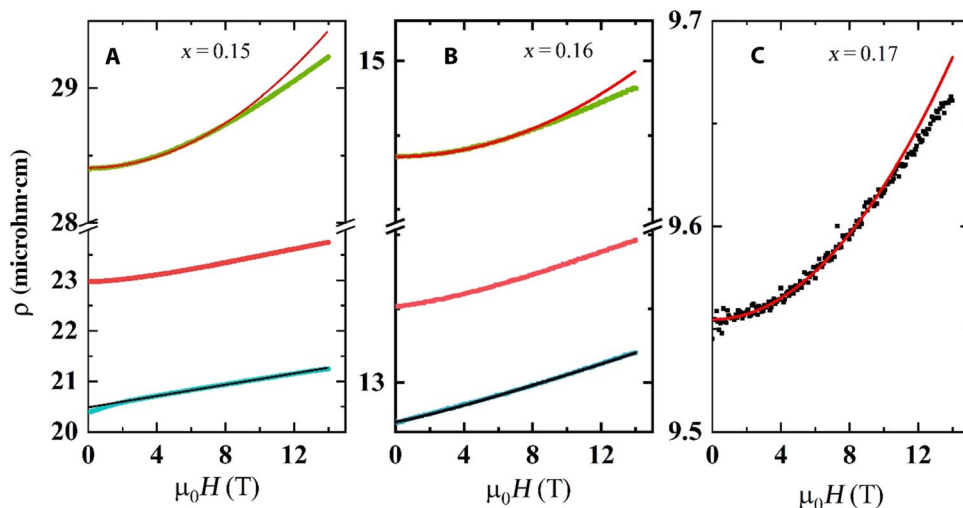


**Fig. 2. MR versus doping.** *ab*-plane resistivity versus transverse magnetic field ( $H//c$  axis) as a function of temperature (color lines) for  $x = 0.15$  (20, 30, and 50 K),  $x = 0.16$  (20, 30, and 40 K), and  $x = 0.17$  (15 K). The fit  $\rho(H) = \rho(0) + C(x)(\mu_0 H)^n$ , where  $n = 1$  for 0.15 (20 K) and  $n = 1.13$  for 0.16 (20 K) (black solid line), and  $\rho(H) = \rho(0) + K(x)(\mu_0 H)^2$  (red solid line) for  $x = 0.15$  (50 K),  $x = 0.16$  (40 K), and  $x = 0.17$  (15 K).

error] in the normal state of the  $x = 0.15$  film. The data show a scaling with  $\Delta\rho/T = (\alpha + \beta(\mu_0 H/T)^m)$  ( $m = 1.09 \pm 0.01$ ), where  $\alpha$  and  $\beta$  are the fitting parameters. Taking  $m = 1$  at low temperatures (below  $<30$  K), we can write  $\Delta\rho = \alpha T + \beta\mu_0 H$ . Converting to energy units, we write  $\Delta\rho \propto (A(x)k_B T + C(x)\mu_B\mu_0 H) \equiv \varepsilon(T, H)$  with  $\varepsilon(T, H)$ , the sum of thermal energy and magnetic field energy. Figure 5B shows all the magnetotransport data as a function of  $\varepsilon(T, H)$ , where  $k_B$  is Boltzmann constant,  $\mu_B$  is the Bohr magneton,  $A$  (2.3 microhm-cm/meV; see Fig. 4C) is the rate of change of resistivity as a function of temperature from Fig. 4B, and  $C$  (0.5 microhm-cm/meV at 0.4 K; see Fig. 4C) is the rate of change of resistivity as a function of magnetic field from Fig. 4A. This scaling is seen in  $x = 0.16$  and  $0.17$  as well (see fig. S3). This means that the resistivity is linear with energy scale  $\varepsilon(T, H)$  at low temperatures for doping between the putative QCP ( $x = 0.14$ ) and the end of the SC dome. This strongly suggests that there is a scale-invariant quantum critical region and that the  $H$ -linear resistivity behavior has the same origin as the  $T$ -linear resistivity behavior. The region of scale invariance is schematically shown in the inset of Fig. 5B. Note that this scaling is different from that of scaling performed in (24). At low temperatures, the LCCO resistivity,  $\rho(T, H)$ , is a linear function of temperature and field. In contrast, in the scaling performed in (24), the resistivity is a nonlinear function of temperature and field.

In LCCO, we know that there is an FSR at  $x = 0.14$  (19) presumably caused by the end of AFM order. If the fluctuations associated with a QCP are responsible for the anomalous low-temperature  $\rho \sim T$  and  $\Delta\rho \sim H$  in LCCO, then our data suggest that there is a quantum critical

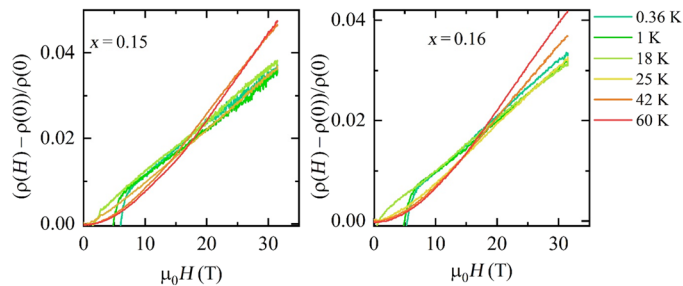


**Fig. 3. High-field MR.**  $ab$ -plane transverse MR ( $\frac{\rho(H) - \rho(0)}{\rho(0)}$ ) for doping  $x = 0.15$  and  $0.16$  measured up to dc field of 31 T. The  $\rho(0)$  is deduced from the extrapolated linear fit to  $H = 0$ .

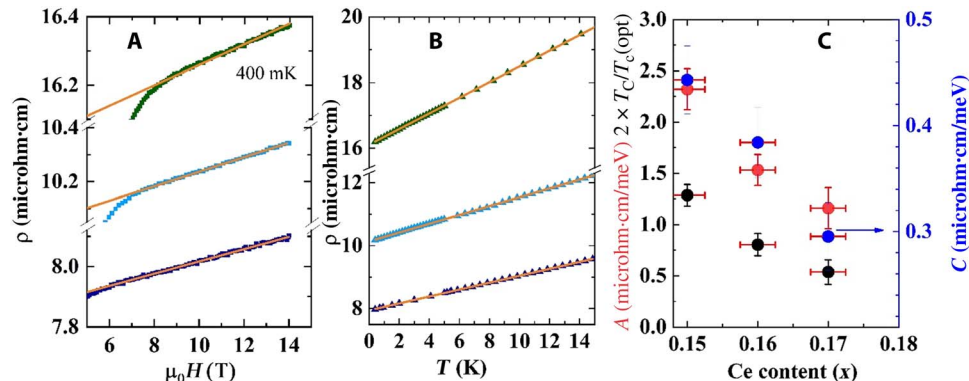


**Fig. 4. Doping-dependent resistivity.** (A)  $ab$ -plane resistivity versus magnetic field ( $H/c$  axis) for LCCO thin films with  $x = 0.15, 0.16,$  and  $0.17$  at 400 mK fitted with  $\rho(H) = \rho(0) + C(x)(\mu_0 H)$  (solid orange line). (B)  $ab$ -plane resistivity versus temperature ( $T$ ) in the field-driven normal state for  $x = 0.15$  (8 T),  $x = 0.16$  (7 T), and  $x = 0.17$  (6 T) fitted with  $\rho(T) = \rho(0) + A(x)T$  (solid orange line). (C) Slope of  $T$  resistivity [ $A(x)$ ; red], magnitude of  $\mu_0 H$  [ $C(x)$ ; blue] from (A) and (B), and normalized  $2 \times T_c$  with respect to optimal  $T_c$  (black) versus doping with respective statistical error of three samples for each doping.

region (not just a point) from  $x = 0.14$  to the end of the SC dome at  $x_c \sim 0.175$ . As shown in Fig. 4, the resistivity coefficient  $A(x)$  of temperature and the resistivity coefficient  $C(x)$  of magnetic field, obtained from fits to the linear temperature and magnetic field resistivity, decrease with  $T_c$  as  $x$  is increased and approach zero at the end of the SC dome. This unique trend of the resistivity coefficients strongly suggests that  $T_c$  and the anomalous scattering are linked to each other.

There are several proposed origins of a linear-in- $H$  MR when  $\omega_c\tau < 1$  (25–27). The low-temperature linear MR is independent of temperature as shown in Figs. 1 and 2 and is supported by the scaling (Fig. 5). At higher temperatures, the magnitude of the  $H^2$  MR decreases with temperature (see Fig. 3 and fig. S1). In contrast, the high-field MR increases with temperature (see Fig. 3). This unusual behavior is consistent with a breakdown of weak-field magnetotransport ( $\delta\rho/\rho(0) \propto H^2$ ) at low temperatures near a QCP (26). This model predicts linear-in- $H$  behavior at the QCP, which is consistent with our experimental data, this model does not explain the high-temperature MR, which needs future study beyond the scope of this work.

We note that a linear-in-field MR has just been reported in the hole-doped cuprate  $\text{La}_{2-x}\text{Sr}_x\text{CuO}_4$  (LSCO) (28) but for a rather different doping, magnetic field, and temperature range than for our results reported here for n-type LCCO. The LSCO data are at higher fields and temperatures [where  $\omega_c\tau \approx 1$  at 20 T (29)], and for doping below the putative QCP, in the region where the FS reconstructed and the normal-state resistivity has an upturn at low temperatures (30). Other magnetoresistivity measurements on LSCO for doping above the QCP have found both  $T$ -linear and  $T^2$  resistivity and an  $H^2$  MR (31). Note that linear in  $H$  is not unusual at high field in a disordered system (27, 29). However, it is quite unusual to see temperature-independent MR at low temperatures and weak field. Thus, the question of whether the superconductivity in n- and p-type cuprates comes from similar normal states will have to await lower-temperature normal-state measurements for the p-type.

The linear-in- $T$  resistivity in both p- and n-type cuprates has recently been attributed to Planckian dissipation (7), i.e., a maximum inelastic relaxation rate,  $\frac{\hbar}{\tau}$ , given by  $k_B T$  (16, 17). This idea appears to be inconsistent with the resistivity behavior of LCCO and other n-type cuprates because the scattering rate goes well beyond the Planckian  $k_B T$  limit above  $\sim 40$  K (3, 14). The linear-in- $T$  resistivity behavior is only

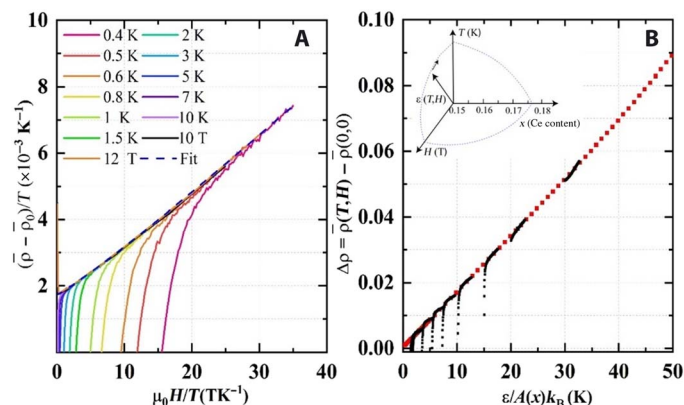


**Fig. 5. Scaling between field and temperature for doping  $x = 0.15$ .** (A)  $(\bar{\rho} - \bar{\rho}(0))/T$  (where  $\bar{\rho} = \rho(T)/\rho(200 \text{ K})$  and  $\bar{\rho}(0) = \frac{\rho(0,0.4)}{\rho(0,200)}$ , taken from Fig. 4A) versus  $\frac{\mu_0 H}{T}$ . This plot has been deduced by varying temperature at a fixed field and by varying field at a fixed temperature (color solid lines). This plot is fitted with  $\Delta\rho = \alpha + \beta(\mu_0 H/T)^m$  ( $m = 1.09$ ) (blue dashed line). (B)  $\bar{\rho}(T, H) - \bar{\rho}(0, 0)$  versus  $T + \frac{C(x)\mu_B}{A(x)k_B}(\mu_0 H) \equiv \epsilon(T, H)/A(x)k_B$  for all MR data (black). The  $\bar{\rho}(0, 0)$  is taken from extrapolating the zero-field resistivity data to  $T = 0$ . The red is the resistivity in 8 T after subtracting the  $\bar{\rho}(0, 8 \text{ T})$ . Inset: Phase diagram in the normal state for overdoped LCCO at low temperatures. The  $x$ - $T$  plane ( $H = 0$ ) is the region where the linear-in- $T$  resistivity is seen. The  $x$ - $H$  plane ( $T = 0$ ) is where the linear MR is seen at low temperatures. The  $\epsilon(T, H)$  is the energy scale below which linear resistivity is found (dashed line).

found below  $\sim 40 \text{ K}$  in the n-type cuprates and increases roughly as  $T^2$  above that temperature up to 400 to 800 K (14). In (16), Hartnoll states that Planckian (nonquasiparticle or incoherent) transport is expected to manifest only at high temperatures [where, roughly, electron  $l_{\text{mfp}}$  (mean free path)  $\sim$  lattice constant]. Evidence for this behavior has been found above  $\sim 250 \text{ K}$  in NCCO and  $\text{Sm}_{2-x}\text{Ce}_x\text{CuO}_4$  crystals via thermal diffusivity measurements (15) and in LCCO from resistivity measurements (14). To our knowledge, there is no agreed upon prediction for the field dependence of the resistivity in the Planckian dissipation limit.

In summary, we have found an unconventional linear-in-field MR at low temperatures and low fields in the electron-doped cuprate LCCO. This behavior is found over an extended doping regime above the purported QCP (i.e., the FSR doping). The magnitude of the linear-in- $H$  resistivity mirrors the magnitude and doping evolution of the linear-in- $T$  resistivity, with both going to zero at the end of the SC dome. An  $H/T$  scaling suggests that there is an energy scale, common to both field and temperature, which is linked to the superconductivity. Moreover, these new results suggest an anomalous quantum criticality in LCCO where the so-called strange-metal state of the cuprates can extend to very low temperatures and fields and over a wide range of doping.

## MATERIALS AND METHODS

The measurements were performed on LCCO films for  $x = 0.13, 0.15, 0.16, 0.17,$  and  $0.18$  compositions. High-quality LCCO films (thickness of about 150 to 200 nm) were grown by the pulsed laser deposition technique on  $\text{SrTiO}_3$  [100] substrates (5 mm by 5 mm) at a temperature of  $750^\circ\text{C}$  with a KrF excimer laser. The films were post-annealed for 40 min at  $2 \times 10^{-5}$  torr oxygen partial pressure at temperatures between  $580^\circ$  and  $640^\circ\text{C}$ . The targets of LCCO were prepared by the solid-state reaction method with 99.999% pure

$\text{La}_2\text{O}_5$ ,  $\text{CeO}_5$ , and  $\text{CuO}$  powders. The Bruker x-ray diffraction of the films shows the  $c$  axis-oriented epitaxial LCCO tetragonal phase. The thickness of the films was determined by cross-sectional scanning electron microscopy. The resistivity measurements of the films were carried out at 400 mK to 200 K in dc magnetic fields up to  $\pm 14 \text{ T}$  in a Quantum Design Physical Property Measurement System with same pattern geometry for all the samples. The Hall component in the MR was removed by adding positive sweep and negative sweep and dividing by 2. In some films, the measurement was performed up to 65 T. The high-field 65-T measurement was performed by standard four-probe ac lock-in method at the National High Magnetic Field Laboratory (NHMFL) Pulsed Field Facility, Los Alamos National Laboratory. The 31-T dc field measurements were performed at NHMFL, Florida State University, Tallahassee.

## SUPPLEMENTARY MATERIALS

Supplementary material for this article is available at <http://advances.sciencemag.org/cgi/content/full/5/5/eaav6753/DC1>

- High-temperature MR
- Temperature-dependent resistivity
- Scaling between temperature and magnetic field
- Resistivity below the FSR
- Pulsed field MR
- MR of an overdoped, non-SC, sample
- Fig. S1. MR versus doping at high temperatures.
- Fig. S2. Derivative of normal-state resistance.
- Fig. S3. Scaling between field and temperature.
- Fig. S4. Resistivity versus temperature and field for  $x = 0.13$ .
- Fig. S5. High-field MR of  $x = 0.15$ .
- Fig. S6. MR for  $x = 0.18$ .

## REFERENCES AND NOTES

1. B. Keimer, S. A. Kivelson, M. R. Norman, S. Uchida, J. Zaanen, From quantum matter to high-temperature superconductivity in copper oxides. *Nature* **518**, 179–186 (2015).
2. S. Sachdev, B. Keimer, Quantum criticality. *Phys. Today* **64**, 29 (2011).
3. N. P. Armitage, P. Fournier, R. L. Greene, Progress and perspectives on electron-doped cuprates. *Rev. Mod. Phys.* **82**, 2421–2487 (2010).
4. Y. Dagan, M. M. Qazilbash, C. P. Hill, V. N. Kulkarni, R. L. Greene, Evidence for a quantum phase transition in  $\text{Pr}_{2-x}\text{Ce}_x\text{CuO}_{4-\delta}$  from transport measurements. *Phys. Rev. Lett.* **92**, 167001 (2004).
5. S. Badoux, W. Tabis, F. Laliberté, G. Grissonnanche, B. Vignolle, D. Vignolles, J. Béard, D. A. Bonn, W. N. Hardy, R. Liang, N. Doiron-Leyraud, L. Taillefer, C. Proust, Change of carrier density at the pseudogap critical point of a cuprate superconductor. *Nature* **531**, 210–214 (2016).
6. B. J. Ramshaw, S. E. Sebastian, R. D. McDonald, J. Day, B. S. Tan, Z. Zhu, J. B. Betts, R. Liang, D. A. Bonn, W. N. Hardy, N. Harrison, Quasiparticle mass enhancement approaching optimal doping in a high- $T_c$  superconductor. *Science* **348**, 317–320 (2015).
7. A. Legros, S. Benhabib, W. Tabis, F. Laliberté, M. Dion, M. Lizaire, B. Vignolle, D. Vignolles, H. Raffy, Z. Z. Li, P. Auban-Senzier, N. Doiron-Leyraud, P. Fournier, D. Colson, L. Taillefer, C. Proust, Universal  $T$ -linear resistivity and Planckian limit in overdoped cuprates. *Nat. Phys.* **15**, 142–147 (2019).
8. B. Vignolle, A. Carrington, R. A. Cooper, M. M. J. French, A. P. Mackenzie, C. Jaudet, D. Vignolles, C. Proust, N. E. Hussey, Quantum oscillations in an overdoped high- $T_c$  superconductor. *Nature* **455**, 952–955 (2008).
9. N. Doiron-Leyraud, C. Proust, D. LeBoeuf, J. Levallois, J.-B. Bonnemaïson, R. Liang, D. A. Bonn, W. N. Hardy, L. Taillefer, Quantum oscillations and the Fermi surface in an underdoped high- $T_c$  superconductor. *Nature* **447**, 565–568 (2007).
10. T. Helm, M. V. Kartsovnik, M. Bartkowiak, N. Bittner, M. Lambacher, A. Erb, J. Wosnitzer, R. Gross, Evolution of the fermi surface of the electron-doped high-temperature superconductor  $\text{Nd}_{2-x}\text{Ce}_x\text{CuO}_4$  revealed by Shubnikov-de Haas oscillations. *Phys. Rev. Lett.* **103**, 157002 (2009).
11. J. Lin, A. J. Millis, Theory of low-temperature Hall effect in electron-doped cuprates. *Phys. Rev. B* **72**, 214506 (2005).
12. O. Gunnarsson, M. Calandra, J. E. Han, *Colloquium: Saturation of electrical resistivity*. *Rev. Mod. Phys.* **75**, 1085–1099 (2003).

13. P. L. Bach, S. R. Saha, K. Kirshenbaum, J. Paglione, R. L. Greene, High-temperature resistivity in the iron pnictides and the electron-doped cuprates. *Phys. Rev. B* **83**, 212506 (2011).
14. T. Sarkar, R. L. Greene, S. Das Sarma, Anomalous normal state resistivity in superconducting  $\text{La}_{2-x}\text{Ce}_x\text{CuO}_4$ : Fermi liquid or strange metal? *Phys. Rev. B* **98**, 224503 (2018).
15. J. Zhang, E. D. Kountz, E. M. Levenson-Falk, D. Song, R. L. Greene, A. Kapitulnik, Thermal diffusivity above the Mott-Ioffe-Regel limit. arXiv:1808.07564 [cond-mat.str-el] (22 August 2018).
16. S. A. Hartnoll, Theory of universal incoherent metallic transport. *Nat. Phys.* **11**, 54–61 (2015).
17. J. Zaanen, Why the temperature is high. *Nature* **430**, 512–513 (2004).
18. P. R. Mandal, T. Sarkar, J. S. Higgins, R. L. Greene, Nernst effect in the electron-doped cuprate superconductor  $\text{La}_{2-x}\text{Ce}_x\text{CuO}_4$ . *Phys. Rev. B* **97**, 014522 (2018).
19. T. Sarkar, P. R. Mandal, J. S. Higgins, Y. Zhao, H. Yu, K. Jin, R. L. Greene, Fermi surface reconstruction and anomalous low-temperature resistivity in electron-doped  $\text{La}_{2-x}\text{Ce}_x\text{CuO}_4$ . *Phys. Rev. B* **96**, 155449 (2017).
20. H. Matsui, T. Takahashi, T. Sato, K. Terashima, H. Ding, T. Uefuji, K. Yamada, Evolution of the pseudogap across the magnet-superconductor phase boundary of  $\text{Nd}_{2-x}\text{Ce}_x\text{CuO}_4$ . *Phys. Rev. B* **75**, 224514 (2007).
21. J. S. Higgins, M. K. Chan, T. Sarkar, R. D. McDonald, R. L. Greene, N. P. Butch, Quantum oscillations from the reconstructed Fermi surface in electron-doped cuprate superconductors. *New J. Phys.* **20**, 043019 (2018).
22. K. Jin, N. P. Butch, K. Kirshenbaum, J. Paglione, R. L. Greene, Link between spin fluctuations and electron pairing in copper oxide superconductors. *Nature* **476**, 73–75 (2011).
23. A. B. Pippard, *Magnetoconductance in Metals* (Cambridge Univ. Press, 2009).
24. I. M. Hayes, R. D. McDonald, N. P. Breznay, T. Helm, P. J. W. Moll, M. Wartenbe, A. Shekhter, J. G. Analytis, Scaling between magnetic field and temperature in the high-temperature superconductor  $\text{BaFe}_2(\text{As}_{1-x}\text{P}_x)_2$ . *Nat. Phys.* **12**, 916–919 (2016).
25. A. E. Koshelev, Linear magnetoconductivity in multiband spin-density-wave metals with nonideal nesting. *Phys. Rev. B* **88**, 060412(R) (2013).
26. J. Fenton, A. J. Schofield, Breakdown of weak-field magnetotransport at a metallic quantum critical point. *Phys. Rev. Lett.* **95**, 247201 (2005).
27. A. A. Patel, J. McGreevy, D. P. Arovas, S. Sachdev, Magnetotransport in a model of a disordered strange metal. *Phys. Rev. X* **8**, 021049 (2018).
28. P. Giraldo-Gallo, J. A. Galvis, Z. Stegen, K. A. Modic, F. F. Balakirev, J. B. Betts, X. Lian, C. Moir, S. C. Riggs, J. Wu, A. T. Bollinger, X. He, I. Božović, B. J. Ramshaw, R. D. McDonald, G. S. Boebinger, A. Shekhter, Scale-invariant magnetoresistance in a cuprate superconductor. *Science* **361**, 479–481 (2018).
29. J. Singleton, A simple transport model for the temperature-dependent linear magnetoresistance of high-temperature superconductors. arXiv:1810.01998v1 [cond-mat.supr-con] (3 October 2018).
30. F. Laliberté, W. Tabis, S. Badoux, B. Vignolle, D. Destraz, N. Momono, T. Kurosawa, K. Yamada, H. Takagi, N. Doiron-Leyraud, C. Proust, L. Taillefer, Origin of the metal-to-insulator crossover in cuprate superconductors. arXiv:1606.04491 [cond-mat.supr-con] (14 June 2016).
31. R. A. Cooper, Y. Wang, B. Vignolle, O. J. Lipscombe, S. M. Hayden, Y. Tanabe, T. Adachi, Y. Koike, M. Nohara, H. Takagi, C. Proust, N. E. Hussey, Anomalous criticality in the electrical resistivity of  $\text{La}_{2-x}\text{Sr}_x\text{CuO}_4$ . *Science* **323**, 603–607 (2009).

**Acknowledgments:** We thank J. Paglione, N. Butch, and S. Das Sarma for discussions and comments on the manuscript. We thank W. Coniglio for help with the 31-T measurement. We also thank J. Higgins for advice and help with some of the measurements. **Funding:** This work was supported by the NSF under grant no. DMR-1708334 and the Maryland Center for Nanophysics and Advanced Materials (CNAM). The National High Magnetic Field Laboratory was supported by the NSF Cooperative agreement nos. DMR-1157490 and DMR-1644779, the state of Florida, and the U.S. Department of Energy. High magnetic field measurements at Los Alamos National Laboratory were supported by DOE-BES Science at 100T grant. **Author contributions:** R.L.G. conceived and directed the project. T.S. performed the analysis. T.S., P.R.M., and N.R.P. prepared the samples and performed the measurements. T.S. and M.K.C. performed the high magnetic field measurements. R.L.G. and T.S. wrote the manuscript and discussed with all other authors. **Competing interests:** The authors declare that they have no competing interests. **Data and materials availability:** All data needed to evaluate the conclusions in the paper are present in the paper and/or the Supplementary Materials. Additional data related to this paper may be requested from the authors. Correspondence and requests for materials should be addressed to R.L.G.

Submitted 9 October 2018

Accepted 2 April 2019

Published 17 May 2019

10.1126/sciadv.aav6753

**Citation:** T. Sarkar, P. R. Mandal, N. R. Poniatowski, M. K. Chan, R. L. Greene, Correlation between scale-invariant normal-state resistivity and superconductivity in an electron-doped cuprate. *Sci. Adv.* **5**, eaav6753 (2019).